Robust INS/GPS Sensor Fusion for UAV Localization Using SDRE Nonlinear Filtering

Abdelkrim Nemra and Nabil Aouf

***Abstract*—The aim of this paper is to present a new INS/GPS sensor fusion scheme, based on State-Dependent Riccati Equation (SDRE) nonlinear filtering, for Unmanned Aerial Vehicle (UAV) localization problem. SDRE navigation filter is proposed as an alternative to Extended Kalman Filter (EKF), which has been largely used in the literature. Based on optimal control theory, SDRE filter solves issues linked with EKF filter such as linearization errors, which severely decrease UAV localization performances. Stability proof of SDRE nonlinear filter is also presented and validated on a 3-D UAV flight scenario. Results obtained by SDRE navigation filter were compared to EKF navigation filter results. This comparison shows better UAV localization performance using SDRE filter. The suitability of the SDRE navigation filter over an unscented Kalman navigation filter for highly nonlinear UAV flights is also demonstrated.**

***Index Terms*—Sensor data fusion, state-dependent Riccati equation (SDRE) nonlinear filter, SDRE stability, unmanned aerial vehicle (UAV) localization.**

I. Introduction

OVER the last few years, Unmanned Aerial Vehicles (UAVs) have attracted attention in a number of civilian and military applications. They are able to perform tasks in highly hostile environments, where access to humans is limited. For these autonomous aerial vehicles, precise navigation is crucial in order to achieve high-performance flights. Several sensing systems are used in UAV navigation such as: inertial navigation systems (INS), global positioning systems (GPSs), air-data dead reckoning systems, radio navigation systems, and Doppler heading reference systems.

INS is the most used navigation sensor providing UAV position, velocity and attitude. However, it has small bias errors, which are continuously increasing with time. Hence, additional aerial vehicle position information from an accurate navigation sensor, such as GPS system, is required. GPS sensor will help to estimate the INS bias errors using a navigation filter, which will then give improved UAV position.

Nowadays, fusing data from different sensors to improve performance of the overall sensing system becomes necessary in various applications. For aerial navigation, fusion of GPS measurements with INS measurements by means of filtering techniques is vital to deliver the level of localization precision required by UAV missions.

Currently, the most used technique to fuse navigation data is Kalman filter [1]. Although Kalman filter is capable of providing real-time vehicle position updates, it is based on linear system models and it suffers from linearization when dealing with nonlinear models. In this case, an Extended Kalman Filter (EKF) is adopted [2], where by means of Taylor series expansion, the nonlinear system is linearized and approximated around each current state estimate. Linear Kalman filter is then applied to produce the next state estimate. When large deviations between the estimated state trajectory and the nominal trajectory exist, the nonlinear model is weakly approximated by Taylor series expansion around the conditional mean. This makes high-order terms of Taylor series expansion necessary. However, in the EKF, these high-order terms are neglected.

Other data fusion techniques based on probabilistic approaches were presented and used in the literature. One of these techniques is Particle Filter (PF) [3], [4]. The main drawback of this filter is its computational requirement, which makes it not very suitable for real-time applications such as aerial navigation problem. Approaches based on Unscented Transform (UT) resulted in a technique called Unscented Kalman Filter (UKF) [5]. This technique preserves the linear update structure of Kalman filter. It uses only second order system moments, which may not be sufficient for some nonlinear systems. In addition, the number of sigma points, used in UKF, is small and may not represent adequately complicated distributions. Moreover, unscented transformation of the sigma-points is computationally heavy, which is not suitable and practical for real-time aerial navigation applications.

In this paper, we investigate an alternative to EKF-based data fusion technique for UAV localization problem. This alternative is based on INS and GPS data and uses a State-Dependent Riccati Equations (SDRE) nonlinear filtering formulation. SDRE techniques are rapidly emerging as optimal nonlinear control and filtering methods. Over the past several years, various SDRE-based design approaches have been successfully applied to aerospace problems. SDRE-based designs have been used in advanced guidance [6], [7], in output feedback nonlinear $H2$ autopilot [8], and in full information nonlinear $H\infty$ autopilot [9]. Before that, a parameter-dependent Riccati equation technique was used in a pitch-yaw autopilot design where the parameter, roll rate, was exogenously supplied by a roll autopilot [10]. In addition, SDRE-based design approaches have been applied to the control design for a nonlinear benchmark problem [11], [12].

Manuscript received January 30, 2009; revised September 22, 2009; accepted September 22, 2009. Current version published March 10, 2010. The associate editor coordinating the review of this paper and approving it for publication was Prof. Evgeny Katz.

A. Nemra is with the Polytechnic Military School, BP17, Bordj-El-Bahri, Algeiers, Algeria, and also with the Department of Informatics and Sensors, Cranfield University, Shrivenham, SN6 8LA, U.K. (e-mail: karim_nemra@yahoo.fr; a.nemra@cranfield.ac.uk).

N. Aouf is with the Department of Informatics and Sensors, Cranfield University, Shrivenham, SN6 8LA, U.K. (e-mail: n.aouf@cranfield.ac.uk).

Color versions of one or more of the figures in this paper are available online at http://ieeexplore.ieee.org.

Digital Object Identifier 10.1109/JSEN.2009.2034730

In [13], SDRE nonlinear regulation, SDRE nonlinear $H\infty$ and SDRE nonlinear $H2$ design methodologies were defined and the optimality, suboptimality, and stability properties of SDRE nonlinear controllers were discussed. In [14], the SDRE nonlinear filter formulation was introduced and used for a pendulum-tracking problem. From the cited references, we notice that SDRE formulation was used more for control design problems and only a little for filtering problems. Moreover, these filtering problems are often related to small order systems.

The SDRE nonlinear filter is adopted here to avoid system linearization issues linked with the classical Extended Kalman filtering. However, SDRE filter stability is still an open research problem. Only very few papers introduced results on SDRE system stability proofs. These proofs were achieved for low-order closed-loop SDRE controlled systems [15], [16].

Contributions of this paper are mainly the development and validation of an alternative optimal INS/GPS filtering scheme based on SDRE technique for aerial (UAV) navigation problem and the global stability analysis developed for this SDRE nonlinear filtering system. The SDRE nonlinear filtering approach proposed in this work will present new option to aeronautical engineers for precise and real-time aerial navigation. As the increase of autonomy of unmanned aerial vehicle is our interest, the ideal extension of this work is to use the SDRE nonlinear filtering in the simultaneous localization and mapping (SLAM) problem where navigation precision is crucial and where the SDRE stability study could be looked at to provide more consistency to SLAM operations.

This paper is organized as follows: Section II presents the navigation sensors (INS and GPS) used in this aerial localization problem. Section III describes shortly the EKF. A review of the SDRE nonlinear filter, in addition, to its stability proofs are presented in Section IV. In Section V, simulation results of the SDRE nonlinear filter for the UAV localization problem are given and compared with the KF and EKF and UKF results.

II. INS/GPS Navigation

A. INS/GPS Navigation

1) Inertial Navigation System (INS): The localization problem of an airborne system is formulated using the navigation core-sensing device: Inertial Measurement Unit (IMU). This unit measures the airborne platform acceleration (ax, ay, az) and its rotation rates (p, q, r) with high update rates. These measurements are then processed and transformed, at the INS, to provide the airborne platform position (X, Y, Z), velocity (U, V, W), and attitude (ϕ, θ, ψ), Fig. 1.

Let us present the INS with the following nonlinear model:

$$\begin{cases} \dot{x}(t) = f(x(t), u(t), t) \\ y(t) = h(x(t), u(t), t) \end{cases} \tag{1}$$

where x is the state vector. This latter includes the position, the velocity and Euler angles. u represents the IMU outputs (angle rates, and accelerations)

$$x = [X,\ Y,\ Z,\ U,\ V,\ W,\ \phi,\ \theta,\ \psi]^T \tag{2}$$

$$u = [p,\ q,\ r,\ ax,\ ay,\ az]^T. \tag{3}$$

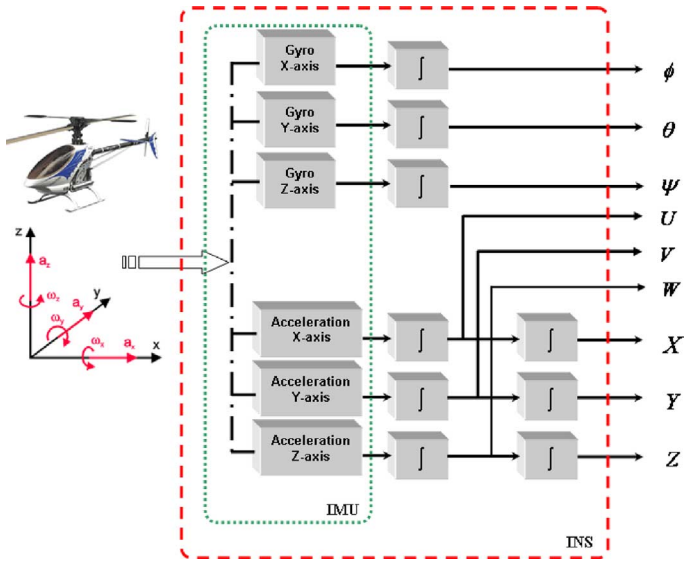

Fig. 1. INS architecture.

The navigation equations require the definition of at least two reference frames. One reference frame is for the body/inertial (vehicle) representation and the other reference frame is for the navigation frame representation. Then, system equations of motion can be given by simple integrations and frame transformations as presented below.

Equations of Motion: Euler angle rates $\dot{\phi}, \dot{\theta}, \dot{\psi}$ can be calculated using the following equation:

$$\begin{bmatrix} \dot{\phi} \\ \dot{\theta} \\ \dot{\psi} \end{bmatrix} = \begin{bmatrix} 1 & \sin(\phi)\tan(\theta) & \cos(\phi)\tan(\theta) \\ 0 & \cos(\phi) & -\sin(\phi) \\ 0 & \sin(\phi)\sec(\theta) & \cos(\phi)\sec(\theta) \end{bmatrix} \begin{bmatrix} p \\ q \\ r \end{bmatrix}. \tag{4}$$

Assuming that the IMU is installed at the vehicle center of gravity, the true vehicle acceleration in the body frame is given by $\dot{U}, \dot{V}, \dot{W}$ as

$$\begin{bmatrix} \dot{U} \\ \dot{V} \\ \dot{W} \end{bmatrix} = \begin{bmatrix} ax + Vr - Wq + g\sin(\theta) \\ ay - Ur + Wp - g\cos(\theta)\sin(\phi) \\ az + Uq - Vp - g\cos(\theta)\cos(\phi) \end{bmatrix}. \tag{5}$$

The resulting acceleration vector is integrated with respect to time to obtain the velocity of the vehicle in the body frame as

$$\begin{bmatrix} U \\ V \\ W \end{bmatrix} = \int \begin{bmatrix} \dot{U} \\ \dot{V} \\ \dot{W} \end{bmatrix} dt. \tag{6}$$

The velocity vector is then integrated to read the position of the vehicle in the body frame. If the velocity is transformed down to the navigation frame and is integrated, we obtain the position vector $[X, Y, Z]^T$ in the navigation frame as

$$\begin{bmatrix} X \\ Y \\ Z \end{bmatrix} = \int C^T bn(\phi, \theta, \psi) \begin{bmatrix} U \\ V \\ W \end{bmatrix} dt \tag{7}$$

where Cbn is the Direct Cosine Transform matrix that rotates a vector from the body frame to the navigation frame shown in

(8) at the bottom of the page. The nonlinear INS state model is given by (9) shown at the bottom of the page. The observation model, related to the UAV position, based on the INS system is given by

$$h(x,u)=\begin{bmatrix}1&0&0&0&0&0&0&0&0\\0&1&0&0&0&0&0&0&0\\0&0&1&0&0&0&0&0&0\end{bmatrix}. \tag{10}$$

The problem with the navigation solution given by INS, Fig. 1, is that it drifts with time as in most other dead reckoning systems. The drift rate of the inertial position is typically a cubic function of time. Small errors in gyros will be accumulated in angle estimates (roll and pitch), which in turn misrepresent gravitational acceleration as the vehicle acceleration and results in quadratic velocity (and cubic position) errors. This makes the development of any inertial only based localization solution very unsuitable. Therefore, INS requires reliable and effective additional information to reduce these errors. The additional source, providing aerial vehicle position, used in this paper is GPS.

INS Errors: Most of INS errors are attributed to the inertial sensors (instrument errors). These are the residual errors exhibited by the installed gyros and accelerometers following calibration of the INS. The dominant error sources of INS system are shown in Table I.

Due to mathematical integration, errors in the accelerations, and angular rates lead to steadily growing errors in position and velocity of the aircraft. These are called navigation errors and there are nine of them – three position errors, three velocity errors, two attitude errors, and one heading error. Gravity model can also cause INS errors, since variations, along the earth and with height, in the acceleration due to gravity are often not modelled accurately. If an unaided INS system is used, these errors grow with time and the INS position will largely drift from the true vehicle position as can be seen in Fig. 13 (red trajectory).

TABLE I
SENSOR ERRORS ININS

INS errors	Impact
Alignment errors	Roll, pitch and heading errors
Accelerometer bias or offset	A constant offset in the accelerometer output that changes randomly after each turn-on
Nonorthogonality of gyros and accelerometers	The accelerometer axes, gyro uncertainty and misalignment
Gyro drift or bias (due to temperature changes)	A constant gyro output without angular rate presence
Gyro scale factor error	Results in an angular rate error proportional to the sensed angular rate
Random noise	Random noise in measurements

2) Global Positioning System (GPS): GPS uses a one-way ranging technique from GPS satellites, which are also broadcasting their estimated positions [17]. Signals from four satellites are used with the user generated replica signal and the measured relative phase. Using triangulation, the location of the receiver can be retrieved [Fig. 2(a)]. Indeed, latitude, longitude, altitude, and a correction to the user's clock are determined using four satellites in an appropriate geometry. The GPS receiver coupled with the computer receiver returns elevation angle and azimuth angle between the user and the satellite. These quantities are measured positive clockwise from the true north, geodetic latitude and longitude of the user. The GPS ranging signal is broadcasted at two frequencies: a primary signal at 1575.42 MHz (L1) and a secondary broadcast at 1227.6 MHz (L2). Civilians use L1 frequency, which has two modulations, viz. C/A or Clear Acquisition Code and P or Precise or Protected Code. C/A is unencrypted signal broadcast at a higher bandwidth and is available only on L1. P code is more precise because it is broadcasted at a higher bandwidth and is restricted for military use. The military operators can degrade the accuracy of the C/A code intentionally and this is known as Selective Availability. If we

$$Cbn=\begin{bmatrix}\mathrm{c}(\theta)\mathrm{c}(\psi) & \mathrm{c}(\theta)\mathrm{s}(\psi) & -\mathrm{s}(\theta)\\ \mathrm{s}(\theta)\mathrm{s}(\phi)\mathrm{c}(\psi)-\mathrm{s}(\psi)\mathrm{c}(\phi) & \mathrm{s}(\psi)\mathrm{s}(\theta)\mathrm{s}(\phi)+\mathrm{c}(\psi)\mathrm{c}(\phi) & \mathrm{s}(\phi)\mathrm{c}(\theta)\\ \mathrm{s}(\theta)\mathrm{c}(\phi)\mathrm{c}(\psi)+\mathrm{s}(\psi)\mathrm{s}(\phi) & \mathrm{s}(\phi)\mathrm{s}(\theta)\mathrm{c}(\phi)-\mathrm{c}(\psi)\mathrm{s}(\theta) & \mathrm{c}(\phi)\mathrm{c}(\theta)\end{bmatrix}. \tag{8}$$

$$f(x,u)=\begin{bmatrix}\begin{bmatrix}\mathrm{c}(\theta)\mathrm{c}(\psi) & \mathrm{c}(\theta)\mathrm{s}(\psi) & -\mathrm{s}(\theta)\\ \mathrm{s}(\theta)\mathrm{s}(\phi)\mathrm{c}(\psi)-\mathrm{s}(\psi)\mathrm{c}(\phi) & \mathrm{s}(\psi)\mathrm{s}(\theta)\mathrm{s}(\phi)+\mathrm{c}(\psi)\mathrm{c}(\phi) & \mathrm{s}(\phi)\mathrm{c}(\theta)\\ \mathrm{s}(\theta)\mathrm{c}(\phi)\mathrm{c}(\psi)+\mathrm{s}(\psi)\mathrm{s}(\phi) & \mathrm{s}(\phi)\mathrm{s}(\theta)\mathrm{c}(\phi)-\mathrm{c}(\psi)\mathrm{s}(\theta) & \mathrm{c}(\phi)\mathrm{c}(\theta)\end{bmatrix}^{T}\begin{bmatrix}U\\V\\W\end{bmatrix}\\ \begin{bmatrix}ax+Vr-Wq+g\mathrm{s}(\theta)\\ ay-Ur+Wp-g\mathrm{c}(\theta)\mathrm{s}(\phi)\\ az+Uq-Vp-g\mathrm{c}(\theta)\mathrm{c}(\phi)\end{bmatrix}\\ \begin{bmatrix}1 & \mathrm{s}(\phi)\tan(\theta) & \mathrm{c}(\phi)\tan(\theta)\\ 0 & \mathrm{c}(\phi) & -\mathrm{s}(\phi)\\ 0 & \mathrm{s}(\phi)\sec(\theta) & \mathrm{c}(\phi)\sec(\theta)\end{bmatrix}\begin{bmatrix}p\\q\\r\end{bmatrix}\end{bmatrix} \tag{9}$$

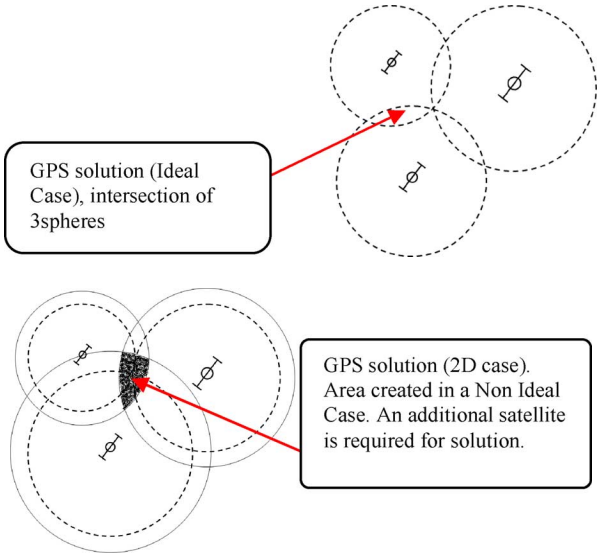

Fig. 2. (a) Ideal case, three intersection spheres. (b) Nonideal case, additional satellite is needed for time offset of the GPS receiver clock.

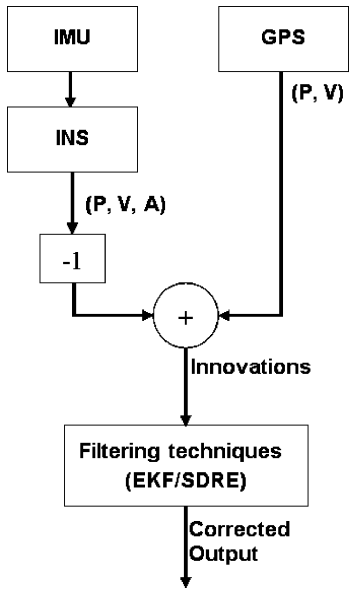

Fig. 3. INS aided GPS sensor fusion.

have a perfect clock in both the satellite and the receiver and if the signal is not affected by noise then precision in calculating the receiver position can be achieved [Fig. 2(a)]. Otherwise, an additional satellite is needed for time offset of the GPS receiver clock [Fig. 2(b)].

In this paper, good precision of GPS signals is assumed. GPS ranging errors, [17], are assumed minimized using additional satellites, if necessary, to correct user's (UAV) clock. Thus, GPS signals are suitable to use in the sensor fusion process with the INS system by means of a navigation-filtering scheme, as illustrated in Fig. 3.

III. Extended Kalman Filter

Based on different estimation models, navigation filters are adopted as a sensor fusion scheme to obtain aerial vehicle states. One of these models, proposed in [1] and [2], is a linear model based on the error navigation model with assumptions on Euler angles (small Euler angles). In this case, a linear Kalman filter is enough to use. However, those assumptions are generally not valid, which makes nonlinear filtering approaches, such as EKF as detailed below, required [2], [18], [19].

Our system, defined in (9) and (10), is converted to a nonlinear discrete time state transition equation using the zero-order hold (ZOH) function

$$\begin{aligned} x_k &= f(x_{k-1}, u_k, w_k) \\ y_k &= h(x_k, v_k) \end{aligned} \tag{11}$$

x_k is the state at time step k, w_k is some additive noise, y_k is the observation made at time k, v_k is some additive observation noise. We assume that w_k and v_k are uncorrelated zero-mean Gaussian with known covariance Q_k and R_k. The objective of the filtering technique is, then, to estimate x_k using available observation y_k.

The nonlinear vehicle model and observation model maybe expanded around the filtered and predicted estimates of $\hat{x}_k$ and $\hat{x}_{k-1}$

$$\begin{aligned} x_k = f(\hat{x}_{k-1/k-1}, u_k) + \Delta f_k(x)\left[x_k - \hat{x}_{k/k}\right] + \\ + \Delta_1\left[x_k - \hat{x}_{k/k}\right] + \left[\Delta f_w(x) + \Delta_2\left[x_k - \hat{x}_{k/k}\right]\right] w_k \end{aligned} \tag{12}$$

$$\begin{aligned} y_k = h(\hat{x}_{k/k-1}, u_k) + \Delta h_k(x)\left[x_k - \hat{x}_{k/k-1}\right] + \\ + \Delta_3\left[x_k - \hat{x}_{k/k-1}\right] + v_k \end{aligned} \tag{13}$$

where $\Delta f_k(x)$ is the Jacobian of f evaluated at x_{k-1}, $\Delta f_w(x)$ the Jacobian of f/w_k evaluated at x_{k-1} and $\Delta h_k(x)$ is the Jacobian of h evaluated at x_{k-1} and $\Delta_{i=1,..3}$ represents higher order terms of the Taylor series expansion.

The filter state error is defined as

$$\tilde{x}_{k/k} = x_k - \hat{x}_{k/k}. \tag{14}$$

The prediction error can be determined by subtracting the true state x_k from the prediction estimate as

$$\widetilde{x}_{k/k-1} = x_k - \hat{x}_{k/k-1}. \tag{15}$$

Neglecting the high-order terms of the Taylor series, the sate and observation models can be rewritten as

$$\begin{aligned} x_{k+1} &= F_k x_k + \Gamma_k w_k \\ y_k &= H_k x_k + v_k \end{aligned} \tag{16}$$

where $Fk = \Delta f_k(\hat{x}_{k/k})$, $\Gamma_k = \Delta f_w(\hat{x}_{k/k})$.

EKF final form is written as a predictor-corrector scheme:

Predictor:

$$\hat{x}_{k+1/k} = f(\hat{x}_{k/k}, u_k, 0) \tag{17}$$

$$P_{k+1/k} = F_k P_{k/k} {F_k}^T + \Gamma_k Q_k \Gamma_k^T. \tag{18}$$

Corrector:

$$\hat{x}_{kk} = \hat{x}_{kk-1} + K_k(y_k - H_k x_{k/k-1}) \tag{19}$$

$$K_k = P_{k/k-1} H_k (H_k P_{k/k-1} {H^T}_k + R_k)^{-1}$$

$$P_{k/k} = P_{k/k-1} - K_k H_k P_{k/k-1}. \tag{20}$$

Unfortunately, when higher order terms of Taylor series are large, the nonlinear model in (11) is poorly approximated by (15), and EKF-based estimation gives poor performances.

IV. SDRE Nonlinear Filter

SDRE techniques are used as control and filtering design methods based on state dependent coefficient (SDC) factorization [14]. In [20] and [21], infinite-horizon nonlinear regulator problem is shown as a generalization of time invariant infinite-horizon linear quadratic regulator problem where all system coefficient matrices are state-dependent. When these coefficient matrices are constant, the nonlinear regulator problem collapses with the linear regulator problem and the SDRE control method collapses with the steady-state linear regulator. Filtering counterpart of the SDRE control algorithm is obtained by taking the dual system of the steady-state linear regulator and then allowing coefficient matrices of the dual system to be state-dependent [21]. The dual of the steady-state linear regulator is the steady-state continuous Kalman observer, which, in the absence of control, reduces to the steady-state continuous Kalman filter [21].

A. State Dependent Coefficient (SDC) Form

Consider the nonlinear system

$$\begin{aligned}\dot{x} &= f(x,u) + \Gamma w \\ y &= h(x,u) + v\end{aligned} \tag{21}$$

w and v are white noises with covariance matrices Q and R, respectively.

There are an infinite number of ways to transform this nonlinear system into an SDC form as

$$\begin{aligned}\dot{x} &= F(x,u)x + \Gamma w \\ y &= H(x,u)x + v\end{aligned} \tag{22}$$

where $f(x,u) = F(x,u)x\ h(x,u) = H(x,u)x$.

We note that the INS estimation model in (9) and (10) falls, by some equation manipulations, into an SDC form. This makes the SDRE filtering a very appealing technique to use for this sensor fusion-based UAV localization problem.

B. SDRE Filter Equations

SDRE filter uses system the SDC form and is given in [15] by

$$\dot{\hat{x}} = F(\hat{x},u)\hat{x} + K_f(\hat{x})\left[y(x) - H(\hat{x},u)\hat{x}\right] \tag{23}$$

where

$$K_f(\hat{x}) = PH^T(\hat{x},u)R^{-1} \tag{24}$$

and P is the positive definite solution of the algebraic Riccati equation

$$\begin{aligned}&F(\hat{x},u)P + PF^T(\hat{x},u) \\ &\quad - PH^T(\hat{x},u)R^{-1}H(\hat{x},u)P + \Gamma Q\Gamma^T = 0.\end{aligned} \tag{25}$$

Properties of SDRE techniques and their proofs are presented in [20] and [13], respectively. Nonlinear functions $f(x,u)$ and $h(x,u)$, in (21), are considered as k1-continuously derivable (i.e., belonging to C^k, $k \geq 1$). In SDC parameterization, $F(x,u)$ and $H(x)$ are assumed to be smooth (*i.e.,* C^k, $k \geq 1$). This assumption is valid in our navigation problem since our SDC state parameters are reasonably slowly varying.

C. SDRE Stability

Global stability of the SDRE nonlinear filter, as opposed to local stability of linear systems, is more difficult to demonstrate since getting stable eigenvalues of the discrete SDRE system at each sampling time does not guarantee global asymptotic stability. To the best of our knowledge, no formal stability proofs of the SDRE nonlinear filter were proposed in the literature. In the following, a method based on Lyapunov approach is developed to provide, with all necessary conditions, the stability region of the SDRE nonlinear filter.

From (23) and (24), we can write

$$\dot{\hat{x}} = F(\hat{x},u)\hat{x} + PH^T(\hat{x},u)R^{-1}\left[y(x) - H(\hat{x},u)\hat{x}\right] \tag{26}$$

$$\begin{aligned}\dot{\hat{x}} &= \left(F(\hat{x},u) - PH^T(\hat{x},u)R^{-1}H(\hat{x},u)\right)\hat{x} \\ &\quad + PH^T(\hat{x},u)R^{-1}y(x).\end{aligned} \tag{27}$$

By proposing a definite positive Lyapunov function $V(\hat{x}) = \hat{x}^T P^{-1}\hat{x} > 0$, the SDRE filter stability is guaranteed iff $\dot{V}(\hat{x}) < 0$, [22].

Using this Lyapunov function, we get: $\dot{V}(\hat{x}) = \dot{\hat{x}}^T P^{-1}\hat{x} + \hat{x}^T P^{-1}\dot{\hat{x}}$. As $\dot{P}^{-1} = 0$ (steady-state problem), then

$$\dot{V}(\hat{x}) = 2\dot{\hat{x}}^T P^{-1}\hat{x}. \tag{28}$$

Replacing (27) in (28), we obtain

$$\begin{aligned}\dot{V}(\hat{x}) = 2[&\hat{x}^T F^T(\hat{x},u)P^{-1}\hat{x} \\ &+\hat{x}^T H^T(\hat{x},u)R^{-1}(y(x) - H(\hat{x},u)\hat{x}].\end{aligned} \tag{29}$$

Thus, $\dot{V}(\hat{x}) < 0 \Leftrightarrow \hat{x}^T F^T(\hat{x},u)P^{-1}\hat{x} < 0$ and $\hat{x}^T H^T(\hat{x},u)R^{-1}\left[y(x) - H(\hat{x},u)\hat{x}\right] < 0$.

Let us start by proving, under which conditions, the first term is defined negative

$$1) \quad \hat{x}^T F^T(\hat{x},u)P^{-1}\hat{x} < 0. \tag{30}$$

Proof: This inequality is equivalent to have $F(\hat{x},u)P^{-1}$ as definite negative. $P^{-1} > 0$ and $F(\hat{x},u)$ is the SDC form of $f(x,u)$ and as mentioned earlier in this paper, SDC forms of a nonlinear function f are not unique. In the following, we propose to derive $F_1(\hat{x},u)$ and $F_2(\hat{x},u)$ as two SDC forms of f.

Then, $F(\hat{x},u,\alpha) = \alpha F_1(\hat{x},u) + (1-\alpha)F_2(\hat{x},u)$, $\alpha \in \Re$ is also an SDC form of f since

$$\begin{aligned}&\left[\alpha F_1(\hat{x},u) + (1-\alpha)F_2(\hat{x},u)\,\hat{x}\right] \\ &\quad = \alpha F_1(\hat{x},u)\hat{x} + (1-\alpha)F_2(\hat{x},u)\hat{x} \\ &\quad = \alpha f(\hat{x},u) + (1-\alpha)f(\hat{x},u) = f(\hat{x},u).\end{aligned}$$

$F(\hat{x},u,\alpha)$ represents an infinite SDC parameterization family. α is proposed as an extra parameter that can be used to build a suitable SDC from an infinite SDC form candidates $F(\hat{x},u,\alpha)$. Using the SDC parameterization form $F(\hat{x},u,\alpha)$ in (30), the

parameter α should be chosen to comply with the first three statements, following, to achieve (30):

$$\begin{aligned}
&\text{if } F_1(\hat{x},u)<0 \quad \text{and} \quad F_2(\hat{x},u)<0\\
&\text{then if} \quad 0<\alpha<1 \Rightarrow F(\hat{x},u)<0\\
&\text{if } F_1(\hat{x},u)<0 \quad \text{and} \quad F_2(\hat{x},u)>0\\
&\text{then if} \quad \alpha>1 \Rightarrow F(\hat{x},u)<0\\
&\text{if } F_1(\hat{x},u)>0 \quad \text{and} \quad F_2(\hat{x},u)<0\\
&\text{then if} \quad \alpha<0 \Rightarrow F(\hat{x},u)<0\\
&\text{if } F_1(\hat{x},u)>0 \quad \text{and} \quad F_2(\hat{x},u)>0\\
&\text{then} \quad \forall\alpha\in\Re \Rightarrow F(\hat{x},u)>0.
\end{aligned}$$

Thus, a good choice of α with two possible SDC forms $F_1(\hat{x},u)$ and $F_2(\hat{x},u)$ assures (30) to be definite negative.

Worth to mention that for a more general case of $k+1$ distinct SDC parameterizations, the dimension of α will be of order k and $F(x,u,\alpha)$ will have the following form:

$$F(x,u,\alpha)=(1-\alpha_k)F_{k+1}(x,u)+\sum_{i=1}^{k}\left(\prod_{j=1}^{k}\alpha_j\right)(1-\alpha_{i-1})F_i(x,u). \quad (31)$$

Let us examine, now, the second term in (29), and see, under which conditions its definite negative property holds

$$2)\quad \hat{x}^T H^T(\hat{x})R^{-1}\left[y(x)-H(\hat{x})\hat{x}\right]<0. \quad (32)$$

The covariance matrix R is assumed diagonal $R = diag(\sigma^2 x,\ \sigma^2 y,\ \sigma^2 z)$. Since system observation is the GPS signal $y(x)=[x_{gps}\ \ y_{gps}\ \ z_{gps}]^T$, which is used by the observation matrix in (10), the inequality (32) becomes

$$\frac{1}{\sigma^2 x}\hat{x}(x_{gps}-\hat{x})+\frac{1}{\sigma^2 y}\hat{y}(y_{gps}-\hat{y})+\frac{1}{\sigma^2 z}\hat{z}(z_{gps}-\hat{z})<0$$
$$\frac{\left(\hat{x}-\frac{x_{gps}}{2}\right)^2}{\sigma^2 x}+\frac{\left(\hat{y}-\frac{y_{gps}}{2}\right)^2}{\sigma^2 y}+\frac{\left(\hat{z}-\frac{z_{gps}}{2}\right)^2}{\sigma^2 z}>D \quad (33)$$

where

$$D=\left(\frac{x_{gps}}{2\sigma x}\right)^2+\left(\frac{y_{gps}}{2\sigma y}\right)^2+\left(\frac{z_{gps}}{2\sigma z}\right)^2. \quad (34)$$

This inequality defines the outside region of an ellipsoid centered at $C=[x_{gps}/2\ \ y_{gps}/2\ \ z_{gps}/2]^T$ and with semi-majors: $r_x=\sigma x.\sqrt{D}$, $r_y=\sigma y.\sqrt{D}$, $r_z=\sigma z.\sqrt{D}$..

If α is chosen properly assuring the definite negative property of the first term of $\dot{V}$ in (30), we can claim that the region, specified by (33) defines the stability region of our SDRE nonlinear filter, as shown in Fig. 4.

Let us now evaluate the stability of the SDRE nonlinear filter if the states of the navigation system get inside the ellipse, which implies that $\dot{V}\geq 0$. In this case and from (28), we get

$$\dot{\hat{x}}^T P^{-1}\hat{x}=\hat{x}^T P^{-1}\dot{\hat{x}}\geq 0. \quad (35)$$

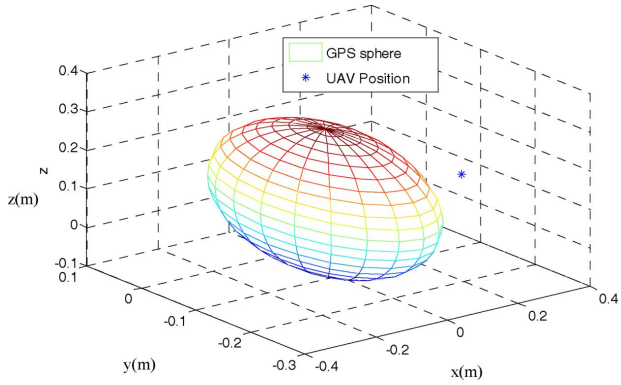

Fig. 4. Ellipsoid region of stability (outside the ellipsoid).

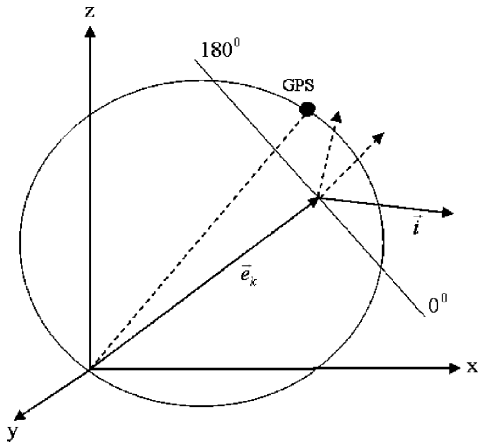

Fig. 5. Stability inside the ellipse.

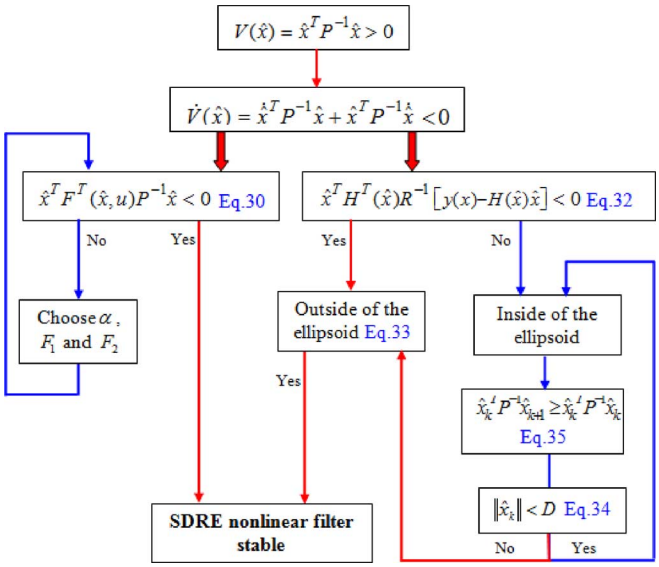

Fig. 6. Proof of stability scheme.

Then, for small values of Δt, we can use numerical derivative to obtain

$$\hat{x}_k^T P^{-1}\left(\frac{\hat{x}_{k+1}-\hat{x}_k}{\Delta t}\right)\geq 0 \quad (36)$$

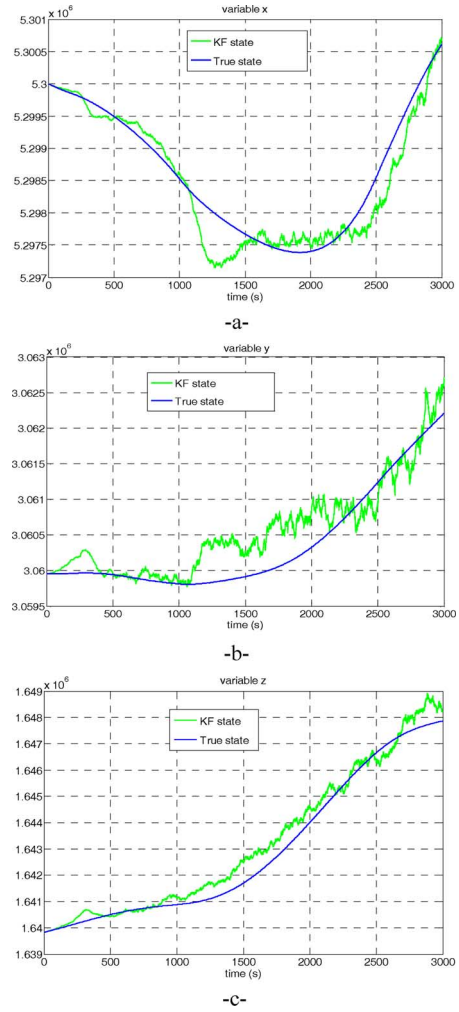

Fig. 7. Estimated position of the airborne, with Kalman filter (linear error model).

$$\hat{x}_k^T P^{-1}(\hat{x}_{k+1} - \hat{x}_k) \geq 0 \tag{37}$$

$$\hat{x}_k^T P^{-1}\hat{x}_{k+1} \geq \hat{x}_k^T P^{-1}\hat{x}_k. \tag{38}$$

To well understand the meaning and the use of these equations, let us represent the inequality (38) by vectors, $\vec{i}$ of coordinates $\hat{x}_k^T P^{-1}$, $\vec{e}_k$ of coordinates $\hat{x}_k$ and $\vec{e}_{k+1}$ of coordinates $\hat{x}_{k+1}$. Then, (38) becomes

$$\vec{i} \cdot \vec{e}_{k+1} \geq \vec{i} \cdot \vec{e}_k. \tag{39}$$

On the other hand, and because $P^{-1} > 0$ and $\hat{x}_k^T P^{-1}\hat{x}_k > 0$, then

$$\vec{i} \cdot \vec{e}_k > 0. \tag{40}$$

This later inequality signifies that $\cos(\vec{i}, \vec{e}_k) > 0$, which means that the angle between $\vec{i}$ and $\vec{e}_k$, is stuck between $]-\pi/2, \pi/2[$, as shown in Fig. 5. Thus, we can state that the vector $\vec{i}$ diverges from the origin and tries to get out of the ellipse.

Combining this result with the inequality (39), we can conclude that the projection of $\vec{e}_{k+1}$ on $\vec{i}$ is larger than the projection of $\vec{e}_k$ on $\vec{i}$, which implies that the vector $\vec{e}_{k+1}$ diverges from the origin more than $\vec{e}_k$. We obtain, then, the following final result.

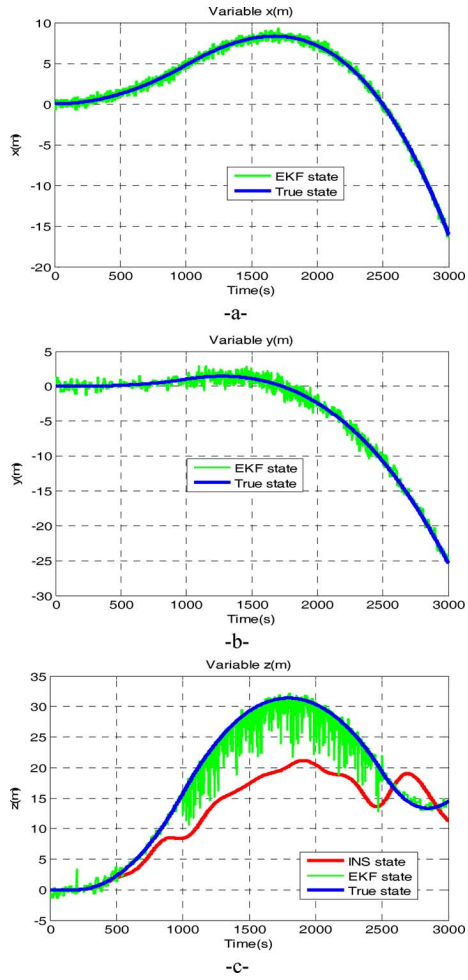

Fig. 8. Estimated position of the airborne, with EKF (linearized model).

$\forall \vec{e}_k\ (\hat{x}_k)$, such that $||\vec{e}_k|| < D$, then $\vec{e}_{k+1}(\vec{x}_{k+1})$ attempts to diverge from the origin, i.e., tries to return back (attraction) to the stability region.

This result shows that, whenever the SDRE filter provides state estimates that bring the system at the frontiers of the inside ellipsoid region, which implies $\dot{V} \geq 0$, and thus no guarantees of the global filter stability, the SDRE nonlinear filter will bring back the system to the region of stability shown in Fig. 4. This way, we showed that the inequality in (32) is globally verified and for the SDRE nonlinear filter stability, a good choice of the parameter α is sufficient to assure it. In Fig. 6, we illustrate graphically the main steps of the SDRE filter stability proof presented above.

V. Simulation Results

We present our simulation results to validate the proposed nonlinear SDRE filter for the autonomous airborne navigation problem. The results of our approach are compared with other navigation filtering approaches. Following are the simulations conducted: firstly, we apply Kalman filter to an INS error model, which is linear under the assumption that Euler angles are small. Then, an EKF is applied to a nonlinear INS model. Last simulations are based on the proposed SDRE nonlinear filter. Comparison of SDRE with UKF navigation results is also highlighted.

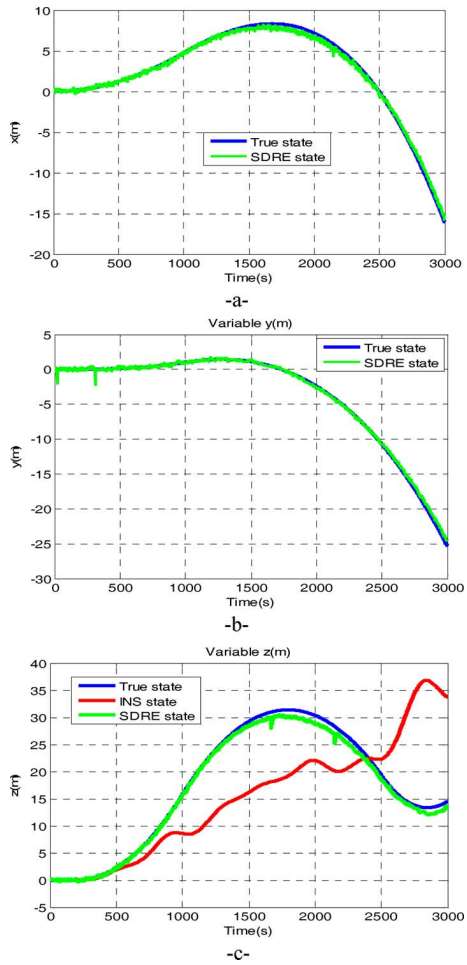

Fig. 9. Estimated position of the airborne, with the SDRE nonlinear filter (nonlinear model).

TABLE II
COMPARISON OF THE STANDARD DEVIATION BETWEEN KF (LINEAR ERROR MODEL), EKF (LINEARIZED MODEL), UKF (NONLINEAR SYSTEM), AND SDRE (NONLINEAR SYSTEM)

	$\sigma_x(m)$	$\sigma_y(m)$	$\sigma_z(m)$
KF	59.0247	23.8104	49.2331
EKF	3.4187	2.9710	7.8191
UKF	3.1234	3.1995	3.5681
SDRE	4.0513	1.2580	3.0705

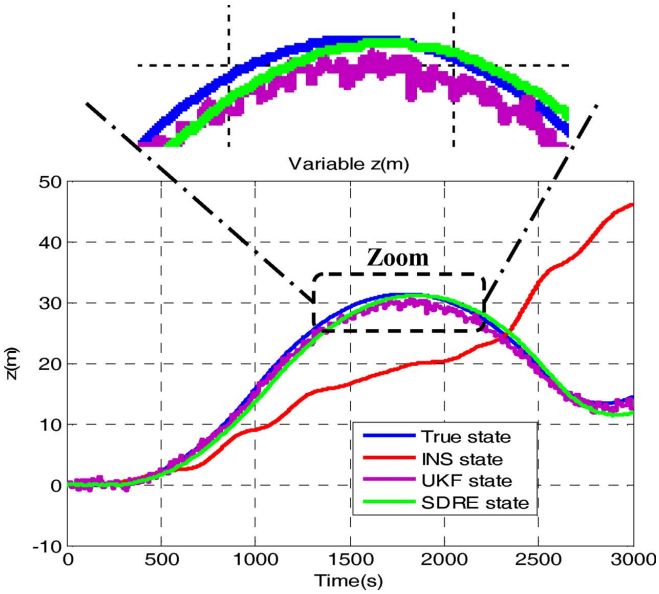

Fig. 10. Estimated of the airborne z position, comparison between UKF and SDRE.

The sampling rates used for each sensor and filter, in this study, are as follows: $f_{\mathrm{INS}} = 100$ Hz, $f_{\mathrm{SDRE}} = 10$ Hz, $f_{\mathrm{EKF}} = 10$ Hz $f_{\mathrm{GPS}} = 1$ Hz

Simulation results shown in Figs. 7–9 represent the estimated UAV position obtained by KF, EKF, and SDRE filters, respectively, for the 3-D trajectory given by Fig. 13.

KF estimation is adequate only for small airborne angular rates. However, if this assumption does not hold, and that is generally the case, then the estimation performance is poor, as presented in Fig. 7.

From Fig. 8(a) and (b), EKF is shown to perform much better than KF for a smooth trajectory. Unfortunately, EKF performance degrades when facing strong nonlinearities. In this case, the Jacobian matrix is ill conditioned, which causes undesirable bumps in the estimated coordinates, as shown in Fig. 8(c) (z variable presents nonlinearities).

Fig. 9 presents the airborne position estimated by SDRE nonlinear filter, which is based on two appropriate SDC forms F_1, F_2 and a suitable value of $\alpha = 0.5$. It is clear that the estimation results are improved with SDRE filter in comparison to KF and EKF filters. We can observe that for strong nonlinearities, the SDRE estimation error increases slightly but it is still within the tolerance for the localization problem in comparison to KF and EKF estimation methods.

Table II shows, for a number of simulation tests, a comparison in terms of standard deviation between the true state and the filter (KF, EKF, UKF, and SDRE) outputs. A better precision of UAV position in the navigation frame is obtained by the SDRE filter with standard deviations $\sigma x = 4.0513$ m $\sigma y = 1.2580$ m $\sigma z = 3.0705$ m after 50 min of navigation. Similar to results in a few recent research on vehicle navigation [23], [24], Table II shows that EKF could lead in few cases to similar results than UKF navigation results. However, UKF is very much more precise than EKF when UAV trajectory is highly nonlinear as in the z-channnel of the proposed simulation example.Table II and Fig. 10 present a comparison between UKF and the nonlinear SDRE filter. As can be seen from Fig. 10, both UKF and SDRE provide good and similar estimations of the UAV z position. Although SDRE results showed a minor improvement over UKF results in Table II, this similarity in performance between SDRE and UKF generally holds. However, UKF filter as expected and as mentioned in the introduction of this paper is computationally heavier (Table III) because of the unscented transformation applied on each sigma-point. From Figs. 10 and 13, we can definitely notice that SDRE estimated trajectory is smoother than the UKF estimated trajectory. This is expected as

TABLE III
COMPARISON OF THE COMPUTATION TIME BETWEEN EKF, UKF, AND SDRE

	EKF	UKF	SDRE
Required time for 100 iterations (s)	0.5670	8.4500	1.5000

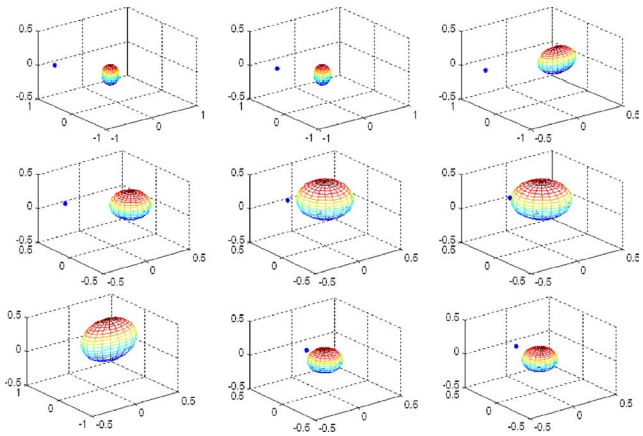

Fig. 11. UAV position and stability region in the navigation frame.

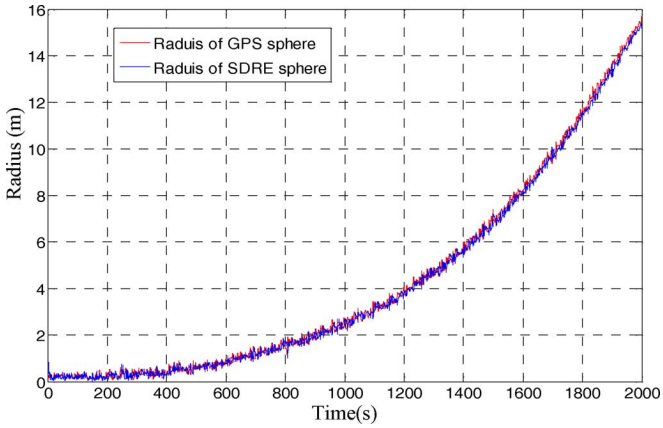

Fig. 12. GPS and SDRE Sphere radius during the time of simulation.

we are dealing with a highly nonlinear navigation system and a sharp UAV trajectory.

In the second part of the simulation, we validate the theoretical stability results obtained in Section IV-C. These results define the exterior of an ellipsoid, (Fig. 4), as the safe and stable flight navigation region for the UAV. As shown in Fig. 11, whenever the UAV is inside or attracted to the GPS ellipsoid (inside the sphere), it is pushed back to remain outside of the ellipsoid to guarantee the stability of the SDRE nonlinear filter. Fig. 12, presents SDRE (blue) and GPS (red) sphere radiuses for the entire simulation time. The convergence of the two radiuses validates the results shown in Fig. 11. Finally, GPS, INS, true and estimated (EKF, UKF, and SDRE) 3-D UAV trajectories are shown in Fig. 13.

VI. CONCLUSION

In this paper, we proposed a State-Dependent Riccati Equation (SDRE) nonlinear filter to estimate the location of an unmanned aerial vehicle (UAV), using INS/GPS data. The proposed method solves issues related to linearization, which poses problem for the classical filtering techniques like the Extended Kalman Filter (EKF). We have compared the performances of our filter with other filters (KF, EKF) performances. Good results were obtained with the SDRE nonlinear filter particularly in the case of strong nonlinearities. Formal proofs of the SDRE nonlinear navigation filter stability were proposed and a stability attractive region was determined.

In our future work we will use the SDRE nonlinear filter to solve the Simultaneous localization and mapping problem of unmanned aerial vehicles with real-time experiments.

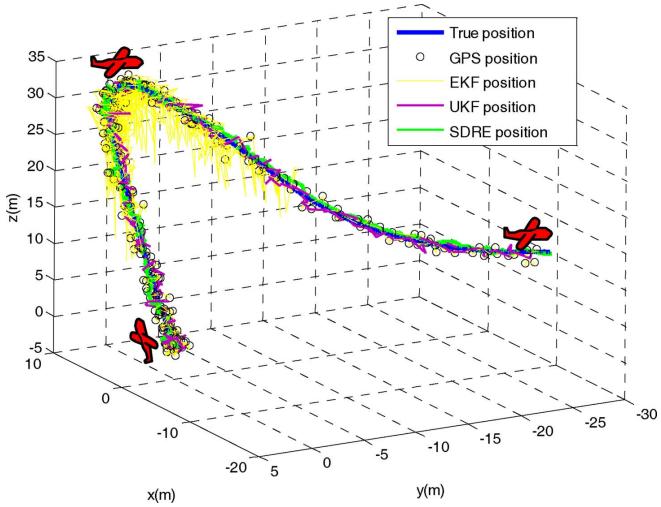

Fig. 13. UAV trajectory and estimated positions.

REFERENCES

[1] V. N. Kumar, *Integration of Inertial Navigation System and Global Positioning System Using Kalman Filtering*. Bombay, Mumbai: Dept. Aerospace Engineering, Indian Institute of Technology, 2004.
[2] S. Ronnback, "Development of an INS/GPS navigation loop for an UAV," M.S. thesis, Lulea Tekniska Universitet, Lulea, Sweden, 2000.
[3] M. K. Pitt and N. Shephard, "Filtering via simulation: Auxiliary particle filters," *J. Amer. Statist. Assoc.*, vol. 94, no. 446, pp. 590–599, 1999.
[4] S. Arulampalam, S. Maskell, N. Gordon, and T. Clapp, "A tutorial on particle filter for on-line nonlinear/non-Gaussian Bayesian tracking," *IEEE Trans. Signal Process.*, vol. 50, no. 2, pp. 174–188, 2002.
[5] S. Julier and J. Uhlmann, "A new extension of the Kalman filter to nonlinear systems," in *Proc. Int Symp. Aerosp./Defense Sensing, Simul. Controls*, Orlando, FL, 1997, vol. 3068, pp. 182–193.
[6] J. R. Cloutier, "Adaptive matched augmented proportional navigation," in *Proc. AIAA Missile Sci. Conf.*, Nov. 1994, pp. 70–79.
[7] J. R. Cloutier, "Time-to-go-less guidance with cross channel couplings," in *Proc. AIAA Missile Sci. Conf.*, Monterey, CA, Dec. 1996.
[8] C. P. Mracek and J. R. Cloutier, "Missile longitudinal autopilot design using the state-dependent Riccati equation method," in *Proc. Int. Conf. Nonlinear Problems in Aviation and Aerospace*, Daytona Beach, FL, May 1996, pp. 387–396.
[9] K. A. Wise, J. L. Sedwick, and R. L. Eberhardt, "Nonlinear control of missiles," McDonnell Douglas Aerospace, MDC 93B0484, 1993.
[10] D. E. Williams, B. F'riedland, and A. N. Madiwale, "Modern control theory for design of autopilots for bankto-turn missiles," *J. Guidance, Control, and Dynamics*, vol. 10, no. 4, pp. 378–386, Jul.-Aug. 1987.
[11] C. P. Mracek and J. R. Cloutier, "A preliminary control design for the nonlinear benchmark problem," in *Proc. IEEE Conf. Control Appl.*, Dearborn, MI, Sep. 1996, pp. 265–272, DOI 10.1109/CCA.1996.558705.
[12] C. P. Mracek and J. R. Cloutier, "Control designs for the nonlinear benchmark problem via the state dependent Riccati equation method," *Int. J. Robust and Nonlinear Control*, vol. 8, pp. 401–433, 1998.

[13] J. R. Cloutier, C. N. D'Souza, and C. P. Mracek, ""Nonlinear regulation and nonlinear H2, control via the state-dependent Riccati equation technique"; Part 1, Theory; Part 2, Examples," in *Proc. Int. Conf. Nonlinear Problems in Aviation and Aerospace*, Daytona Beach, FL, May 1996.

[14] C. P. Mracek, J. R. Cloutier, and C. N. D'Souza, "A new technique for nonlinear estimation," in *Proc. IEEE Conf. Control Appl.*, Dearborn, MI, Sep. 1996, pp. 338–343, DOI 10.1109/CCA.1996.558760.

[15] J. Shamma and J. Cloutier, "Existence of SDRE stabilizing controllers," *IEEE Trans. Autom. Control*, pp. 513–517, Mar. 2003.

[16] J. W. Curtis and R. W. Beard, "Ensuring stability of state-dependent Riccati equation controllers via satisficing," in *Proc. IEEE Conf. Decision Control*, Las Vegas, NV, 2002, vol. 3, pp. 2645–2650.

[17] Parkinson and Spilker, *Global Position System Theory and Application I, II*. Reston, VA: American Institute of Aeronautics and Astronautics, AIAA, 1996.

[18] J. Kim and S. Sukkarieh, "Real-time implementation of airborn inertial-SLAM," in *Robotics and Autonomous Systems*. New York: Elsevier, 2006, vol. 55(2007)62-7, pp. 0921–8890.

[19] G. Mao, S. Drake, and B. D. O. Anderson, *Design of an Extended Kalman Filter for UAV Localisation*. , Australia: Defence Science and Technology Organization (DSTO), 2007, vol. DOI 10.1109/IDC.2007.374554, pp. 224–229.

[20] J. R. Cloutier, "Navigation and control branch U.S. air force armament directorate," in *Proc. Amer. Control Conf.*, Albuquerque, NM, Jun. 1997.

[21] J. R. Cloutier, C. P. Mracek, D. B. Ridgely, and K. D. Hammett, "State-dependent Riccati equation techniques: Theory and applications," in *Proc. Amer. Control Conf. Workshop*, 1998.

[22] D. a. Haessig and B. Friedland, "State dependent differential Riccati equation for nonlinear estimation and control," in *Proc. 15th Triennial World Cong.*, Barcelona, Spain, 2002, IFAC.

[23] C. C. G. Park, K. Kim, and W. Y. Kang, "UKF based in-flight alignment using low cost IMU," in *Proc. AIAA Guidance, Navigation, and Control Conf. Exhibit*, Colorado, USA, 2006, pp. 2006–6353.

[24] A. N. Ndjeng, D. Gruyer, A. Lambert, B. Mourllion, and S. Glaser, "Experimental comparison of Bayesian. Outdoor vehicle localization filters," in *Proc. IEEE ICRA Conf. Workshop on Safe Navigation in Open and Dynamic Environments Application to Autonomous Vehicles*, Kobe, Japan, 2009.

Abdelkrim Nemra received the Engineer degree and the M.S. degree in control systems from the Department of Control, Polytechnic Military School, Algeria, in 2004 and 2006, respectively. Currently, he is working towards the Ph.D. degree at the Department of Informatics and Sensors, Cranfield University, Shrivenham, U.K.

His current research interests include unmanned vehicles, localization of aerial vehicle, and map building. His publications include a number of conference and journal papers in computer vision and data-fusion and a book chapter in robotic.

Nabil Aouf received the Ph.D. degree in control systems from the Department of Electrical Engineering, McGill University, Montreal, Canada, in 2002.

He is a Lecturer at the Department of Informatics and Sensors, Cranfield University, UK. His research interests are aerospace and defence systems, information fusion and vision systems, guidance and navigation, tracking and control and autonomy of systems. He is an Associate Editor of the *International Journal of Computational Intelligence in Control*. He has more than 50 publications of high calibre in his domains of interest.